

Theory and simulation of spin transport in antiferromagnetic semiconductors: Application to MnTeK. Akabli,^{1,2} Y. Magnin,² Masataka Oko,¹ Isao Harada,¹ and H. T. Diep^{2,*}¹*Graduate School of Natural Science and Technology, Okayama University, 3-1-1 Tsushima-naka, Kita-ku, Okayama 700-8530, Japan*²*Laboratoire de Physique Théorique et Modélisation, Université de Cergy-Pontoise, CNRS, UMR 8089 2, Avenue Adolphe Chauvin, FR-95302 Cergy-Pontoise Cedex, France*

(Received 22 May 2010; revised manuscript received 29 December 2010; published 18 July 2011)

In this paper we study the parallel spin current in an antiferromagnetic semiconductor thin film where we take into account the interaction between itinerant spins and lattice spins. The spin model is an anisotropic Heisenberg model. Here we use the Boltzmann equation with numerical data on cluster distribution obtained by Monte Carlo simulations and cluster-construction algorithms. We study the cases of degenerate and nondegenerate semiconductors. The spin resistivity in both cases is shown to depend on the temperature, with a broad maximum at the transition temperature of the lattice spin system. The shape of the maximum depends on the spin anisotropy and on the magnetic field. It shows, however, no sharp peak in contrast to ferromagnetic materials. Our method is applied to MnTe. Comparison to experimental data is given.

DOI: [10.1103/PhysRevB.84.024428](https://doi.org/10.1103/PhysRevB.84.024428)

PACS number(s): 75.76.+j, 05.60.Cd

I. INTRODUCTION

The behavior of the spin resistivity ρ as a function of temperature (T) has been shown and theoretically explained by many authors during the last 50 years. Among the ingredients that govern the properties of ρ , we can mention the scattering of the itinerant spins by the lattice magnons suggested by Kasuya,¹ the diffusion due to impurities,² and the spin-spin correlation.^{3–5} First-principles analysis of spin-disorder resistivity of Fe and Ni has also been recently performed.⁶

Experiments have been performed on many magnetic materials ranging from metals to semiconductors. These results show that the behavior of the spin resistivity depends on the material: some of them show a large peak of ρ at the magnetic transition temperature T_C ,⁷ while others show only a change of slope of ρ giving rise to a peak of the differential resistivity $d\rho/dT$.^{8,9} Very recent experiments such as those performed on ferromagnetic SrRuO₃ thin films,¹⁰ Ru-doped induced ferromagnetic La_{0.4}Ca_{0.6}MnO₃,¹¹ antiferromagnetic ϵ -(Mn_{1-x}Fe_x)_{3.25}Ge,¹² semiconducting Pr_{0.7}Ca_{0.3}MnO₃ thin films,¹³ superconducting BaFe₂As₂ single crystals,¹⁴ La_{1-x}Sr_xMnO₃,¹⁵ and Mn_{1-x}Cr_xTe (Ref. 16) compounds show different forms of anomaly of the magnetic resistivity at the magnetic phase transition temperature.

The magnetic resistivity due to the scattering of itinerant spins by localized lattice spins is proportional to the spin-spin correlation as proposed long ago by De Gennes and Friedel,³ Fisher and Langer,⁴ and recently by Kataoka.⁵ They have shown that changing the range of spin-spin correlation changes the shape of ρ . In a recent work, Zarand *et al.*² showed that in magnetic diluted semiconductors, the shape of the resistivity versus T depends on the interaction between the itinerant spins and localized magnetic impurities, which is characterized by an Anderson localization length ζ . Expressing physical quantities in terms of ζ around impurities, they calculated ρ and showed that its peak height indeed depends on this localization length.

In our previous work^{17–19} we studied the spin current in ferromagnetic thin films. The behavior of the spin resistivity as a function of T has been shown and explained as an effect

of magnetic domains formed in the proximity of the phase transition point. This concept has an advantage over the use of the spin-spin correlation since the distribution of clusters is more easily calculated using Monte Carlo (MC) simulations. Although the formation of spin clusters and their sizes are a consequence of spin-spin correlation, the direct access in numerical calculations to the structure of clusters allows us to study complicated systems such as thin films, systems with impurities, systems with a high degree of instability, etc. On the other hand, the correlation functions are very difficult to calculate. Moreover, as will be shown in this paper, the correlation function cannot be used to explain the behavior of the spin resistivity in antiferromagnets, where very few theoretical investigations have been carried out. One of these is the work by Suezaki and Mori²⁰ which simply predicted that the behavior of the spin resistivity in antiferromagnets is like that in ferromagnets, if the correlation is short ranged. This means that correlation should be limited to “selected nearest neighbors.” Such an explanation is obviously not satisfactory, in particular, when signs of the correlation function between antiparallel spin pairs are taken into account. In a work with a model suitable for magnetic semiconductors, Haas has shown that the resistivity ρ in antiferromagnets is quite different from that of ferromagnets.²¹ In particular, he found that while ferromagnets show a peak of ρ at the magnetic transition of the lattice spins, antiferromagnets do not have such a peak. We will demonstrate that all these effects can be interpreted in terms of clusters used in our model.

In this paper, we introduce a simple model which takes into account the interaction between itinerant spins and localized lattice spins. This is similar to the $s-d$ model.²¹ The lattice spins interact with each other via antiferromagnetic interactions. The model will be studied here by a combination of MC simulation and the Boltzmann equation. As will be discussed below, such a model corresponds to antiferromagnetic semiconductors such as MnTe. An application is made for this compound in the present work.

The paper is organized as follows. In Sec. II, we show and discuss our general model and its application to the antiferromagnetic case using the Boltzmann equation formu-

lated in terms of clusters. We also describe here our MC simulations to obtain the distribution of sizes and number of clusters as functions of T , which will be used to solve the Boltzmann equation. Results on the effects of Ising-like anisotropy and magnetic field, as well as an application to the case of MnTe, is shown in Sec. III. Concluding remarks are given in Sec. IV.

II. THEORY

Briefly, let us recall the principal theoretical models for magnetic resistivity ρ . In magnetic systems, de Gennes and Friedel³ suggested that the magnetic resistivity is proportional to the spin-spin correlation. As a consequence, in ferromagnetically ordered systems, ρ shows a divergence at the transition temperature T_C , similar to the susceptibility. However, in order to explain the finite cusp of ρ experimentally observed in some experiments, Fisher and Langer⁴ suggested taking into account only short-range correlations in the de Gennes-Friedel theory. Kataoka⁵ has followed the same line in proposing a model where he included, in addition to a parameter describing the correlation range, some other parameters describing effects of the magnetic instability, the density of itinerant spins, and the applied magnetic field.

For antiferromagnetic systems, Suezaki and Mori²⁰ proposed a model to explain the anomalous behavior of the resistivity around the Néel temperature. They used the Kubo formula for an $s-d$ Hamiltonian with some approximations to connect the resistivity to the correlation function. However, it is not so easy to resolve the problem. Therefore, the form of the correlation function was just given in the molecular field approximation. They argued that just below the Néel temperature T_N , a long-range correlation appears giving rise to an additional magnetic potential which causes a gap. This gap affects the electron density, which alters the spin resistivity but does not, in their approximation, interfere in the scattering mechanism. They concluded that, under some considerations, the resistivity should have a peak close to the Néel point. This behavior is observed in Cr, α -Mn, and some rare-earth metals. Note, however, that in the approximations used by Haas,²¹ there is no peak predicted. So, the question of the existence of a peak in antiferromagnets remains open.

Following Haas, for semiconductors we use the following interaction:

$$V = - \sum_n J(\vec{r} - \vec{R}_n) \mathbf{s} \cdot \mathbf{S}_n, \quad (1)$$

where $J(\vec{r} - \vec{R}_n)$ is the exchange interaction between an itinerant spin \mathbf{s} at \vec{r} and the lattice spin \mathbf{S}_n at the lattice site \vec{R}_n . In practice, the sum on lattice spins \mathbf{S}_n should be limited at some cut-off distance, as will be discussed later. Haas supposed that V is weak enough to be considered as a perturbation to the lattice Hamiltonian given by Eq. (15) below. This is what we also suppose in the present paper. He applied his model to ferromagnetic doped CdCr₂Se₄ (Refs. 22–24) and antiferromagnetic semiconductors MnTe. Note, however, that the model by Haas, as well as other existing models, cannot treat the case where itinerant spins, due to the interaction between themselves, induce itinerant magnetic ordering such as in (Ga,Mn)As shown by Matsukura *et al.*⁷ Note also that

both the up-spin and down-spin currents are present in the theory but the authors considered only the effect of the up-spin current since the interaction “itinerant spin”-“lattice spin” is ferromagnetic so that the down-spin current is very small. This theory was built in the framework of the relaxation-time approximation of the Boltzmann equation under an electric field. As have De Gennes and Friedel, here Haas used the spin-spin correlation to describe the scattering of itinerant spins by the disorder of the lattice spins. As a result, the model of Haas shows a peak in the ferromagnetic case but no peak in the antiferromagnetic semiconductors. Experimentally, the absence of a peak has been observed in antiferromagnetic LaFeAsO by McGuire *et al.*²⁵ and in CeRhIn₅ by Christianson *et al.*²⁶

A. Boltzmann equation

In the case of Ising spins in a ferromagnet that we studied before,¹⁹ we have made a theory based on the cluster structure of the lattice spins. The cluster distribution was incorporated in the Boltzmann equation. The number of clusters η and their sizes ξ have been numerically determined using the Hoshen-Kopelman algorithm (Sec. II B).²⁷ We work in diffusive regime with approximation of parabolic band and in an $s-d$ model. In this paper we consider that in our range of temperature the Hall resistivity is constant (constant density). To work with the Born approximation we consider a weak potential of interaction between clusters of spin and conduction electrons. We suppose that the lifetime of clusters is larger than the relaxation time. As in our previous paper,¹⁹ in this paper we use the expression of relaxation time obtained from the Boltzmann equation in the following manner. We first write the Boltzmann equation for f , the distribution function of itinerant electrons, in a uniform electric field \mathbf{E} ,

$$\left(\frac{\hbar \mathbf{k} \cdot e \mathbf{E}}{m} \right) \left(\frac{\partial f^0}{\partial \epsilon} \right) = \left(\frac{\partial f}{\partial t} \right)_{\text{coll}}, \quad (2)$$

where f^0 is the equilibrium Fermi-Dirac function, \mathbf{k} is the wave vector, e and m are the electronic charge and mass, respectively, and ϵ is the electron energy. We next use the following relaxation-time approximation:

$$\left(\frac{\partial f_k}{\partial t} \right)_{\text{coll}} = - \left(\frac{f_k^1}{\tau_k} \right), \quad f_k^1 = f_k - f_k^0, \quad (3)$$

where τ_k is the relaxation time. Supposing elastic collisions, i.e., $k = k'$, and using the detailed balance we have

$$\left(\frac{\partial f_k}{\partial t} \right)_{\text{coll}} = \frac{\Omega}{(2\pi)^3} \int [w_{k',k} (f_{k'}^1 - f_k^1)] d\mathbf{k}', \quad (4)$$

where Ω is the system volume and $w_{k',k}$ is the transition probability between \mathbf{k} and \mathbf{k}' . With Eqs. (3) and (4) we find the following well-known expression:

$$\left(\frac{1}{\tau_k} \right) = \frac{\Omega}{(2\pi)^3} \int [w_{k',k} (1 - \cos \theta)] \sin \theta k'^2 dk' d\theta d\phi, \quad (5)$$

where θ and ϕ are the angles formed by \mathbf{k}' with \mathbf{k} , i.e., spherical coordinates with the z axis parallel to \mathbf{k} .

Now, in Eq. (5) we use the ‘‘Fermi golden rule’’ for $\omega_{k,k'}$ and we obtain

$$\frac{1}{\tau_k} = \frac{\Omega}{(2\pi)^3} \int \{\omega_{k,k'}[1 - \cos(\theta)]\} \sin(\theta) k'^2 dk' d\theta d\phi, \quad (6a)$$

$$\omega_{k,k'} = \frac{(2\pi)m}{\hbar^3 k} |\langle k' | J(r) | k \rangle|^2 \delta(k' - k), \quad (6b)$$

where $J(r)$ is the exchange integral between an itinerant spin and a lattice spin, which is given in the scattering potential, Eq. (1). One has

$$J(r) \equiv J(|\vec{r}' - \vec{R}_n|). \quad (7)$$

Note that for simplicity we have supposed here that the interaction potential $J(r)$ depends only on the relative distance $r = |\vec{r}' - \vec{R}_n|$, not on the direction of $\vec{r} - \vec{R}_n$. We suppose in the following, a potential which exponentially decays with distance:

$$J(r) \equiv V_0 e^{-r/\xi}, \quad (8)$$

where V_0 expresses the magnitude of the interaction and ξ is the averaged cluster size. After some algebra, we arrive at the following relaxation time:

$$\frac{1}{\tau_{k_f}} = \frac{32V_0^2 m \pi}{(2k\hbar)^3} \eta \xi^2 \left[1 - \frac{1}{1 + (2\xi k_f)^2} - \frac{(2\xi k_f)^2}{[1 + (2\xi k_f)^2]^2} \right], \quad (9)$$

where k_f is the Fermi wave vector. As noted by Haas,²¹ the mobility is inversely proportional to the susceptibility χ . So, in examining our expression and in using the expression $\chi = \sum \xi^2 \eta(\xi)$,²⁸ where $\eta(\xi)$ is the number of clusters of size ξ , one sees that the first term of the relaxation time is proportional to the susceptibility. The other two terms are the corrections.

The mobility in the x direction is defined by

$$\mu_x = \frac{e\hbar^2}{3m^2} \frac{\sum_k k^2 (\partial f_k^0 / \partial \epsilon) \tau_k}{\sum_k f_k^0}. \quad (10)$$

We resolve the mobility μ_x explicitly in the following two cases.

Degenerate semiconductors:

$$\sum_k f_k^0 = 2\pi \left(\frac{2m}{\hbar^2} \right)^{3/2} \left[\frac{2}{3} \epsilon_f^{3/2} \right], \quad (11a)$$

$$\begin{aligned} \sum_k k^2 (\partial f_k^0 / \partial \epsilon) \tau_k &= 2\pi \left(\frac{2m}{\hbar^2} \right)^{3/2} \frac{\epsilon_f^{1/2}}{D} \left(\frac{2m\epsilon_f}{\hbar^2} \right)^{5/2} \\ &\times \left[\frac{1 + 8m\xi^2 \epsilon_f / \hbar^2}{8m\xi^2 \epsilon_f / \hbar^2} \right]^2, \end{aligned} \quad (11b)$$

where $D = \eta 4V_0^2 m \pi \xi^2 / \hbar^3$. We arrive at the following mobility:

$$\mu_x = \frac{e\hbar^2}{2m^2} \frac{\epsilon_f^{-1}}{D} \left(\frac{2m\epsilon_f}{\hbar^2} \right)^{5/2} \left[\frac{1 + 8m\xi^2 \epsilon_f / \hbar^2}{8m\xi^2 \epsilon_f / \hbar^2} \right]^2, \quad (12a)$$

$$\sigma = ne\mu = \frac{ne^2}{mDk_f} \left[\frac{1 + 4\xi^2 k_f^2}{4\xi^2} \right]^2. \quad (12b)$$

The resistivity is then

$$\rho = \frac{\eta 4V_0^2 m^2 \pi k_f \xi^2}{ne^2 \hbar^3} \left[\frac{4\xi^2}{1 + 4\xi^2 k_f^2} \right]^2. \quad (13)$$

We can check that the right-hand side has the dimension of a resistivity: $([kg][m]^3)/([C]^2[s]) = [\Omega][m]$.

Nondegenerate semiconductors. In this case, $f_k^0 = \exp(-\beta\epsilon_k)$,

$$\sum_k f_k^0 = 2\pi \left(\frac{2m}{\hbar^2} \right)^{3/2} \beta^{-3/2} \sqrt{\pi} / 2, \quad (14a)$$

$$\begin{aligned} \sum_k k^2 (\partial f_k^0 / \partial \epsilon) \tau_k &= 2\pi \left(\frac{2m}{\hbar^2} \right)^{3/2} \frac{1}{2D(4\xi^2)^2 \beta} \left(\frac{2m}{\hbar^2} \right)^{1/2} \\ &\times \left[1 + \frac{2(16m\xi^2)}{\hbar^2 \beta} + \frac{6(8m\xi^2)^2}{\hbar^4 \beta^2} \right], \end{aligned} \quad (14b)$$

$$\begin{aligned} \sigma = ne\mu &= \frac{ne^2 \hbar^2}{m^2 D (4\xi^2)^2 \sqrt{\pi}} \left(\frac{2m\beta}{\hbar^2} \right)^{1/2} \\ &\times \left[1 + \frac{2 \times 16m\xi^2}{\hbar^2 \beta} + \frac{6(8m\xi^2)^2}{\hbar^4 \beta^2} \right], \end{aligned} \quad (14c)$$

$$\rho = \frac{1}{\sigma}, \quad (14d)$$

where $D = \eta 4V_0^2 m \pi \xi^2 / \hbar^3$. Note that the formulation of our theory in terms of cluster number η and cluster size ξ is numerically very convenient. These quantities are easily calculated by MC simulation for the Ising model. The method can be generalized to the case of Heisenberg spins where the calculation is more complicated, as seen below. In Sec. III A we will examine values of parameter V_0 , where the Born approximation is valid.

B. Algorithm of Hoshen-Kopelman and Wolff’s procedure

We use the Heisenberg spin model with an Ising-like anisotropy for an antiferromagnetic film of a body-centered cubic (bcc) lattice of $N_x \times N_y \times N_z$ cells where there are two atoms per cell. The film has two symmetrical (001) surfaces, i.e., surfaces perpendicular to the z direction. We use the periodic boundary conditions in the xy plane and the mirror reflections in the z direction. The lattice Hamiltonian is written as follows:

$$\mathcal{H} = J \sum_{\langle i,j \rangle} \mathbf{S}_i \cdot \mathbf{S}_j + A \sum_{\langle i,j \rangle} S_i^z S_j^z, \quad (15)$$

where \mathbf{S}_i is the Heisenberg spin at site i ; $\sum_{\langle i,j \rangle}$ is performed over all nearest-neighbor (NN) spin pairs. For simplicity, we assume here that all interactions, including those at the two surfaces, are identical: J is positive (antiferromagnetic) and A is an Ising-like anisotropy which is a positive constant. When A is zero, one has the isotropic Heisenberg model, and when $A \rightarrow \infty$, one has the Ising model. The classical Heisenberg spin model is continuous, so it allows the domain walls to be less abrupt, and therefore softens the behavior of the magnetic resistance. Note that for clarity of illustration, in Sec. II B,

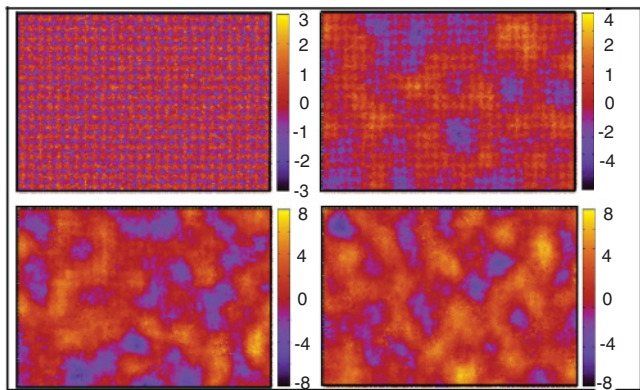


FIG. 1. (Color) Energy map of an itinerant spin in the xy plane with $D_1 = 2$ in units of the lattice constant a and $A = 0.01$, for $T = 0.01$, $T = 1.0$, $T = 2.0$, and $T = 2.5$ (from left to right, top to bottom, respectively). The values of energy corresponding to different colors are given on the right.

we suppose only NN interaction J . In the application to MnTe shown in Sec. III C, the exchange integral is distance dependent and we shall take into account up to the third NN interaction.

Hereafter, the temperature is expressed in units of J/k_B , k_B being the Boltzmann constant. A is given in units of J . The resistivity ρ is shown in atomic units.

For this paper, we use $N_x = N_y = 20$ and $N_z = 8$. The finite-size effect, as well as surface effects, are out of the scope of the present paper. Using the Hamiltonian (15), we equilibrate the lattice at a temperature T by the standard Monte Carlo simulation. In order to analyze the spin resistivity, we should know the energy landscape seen by an itinerant spin. The energy map of an itinerant electron in the lattice is obtained as follows: at each position its energy is calculated using Eq. (8) within a cutoff at a distance $D_1 = 2$ in units of the lattice constant a . The energy value is coded by a color, as shown in Fig. 1 for the case $A = 0.01$. As seen, at very low T ($T = 0.01$), the energy map is periodic just as is the lattice, i.e., no disorder. At $T = 1$, well below the Néel temperature $T_N \simeq 2.3$, we observe an energy map which indicates the existence of many large defect clusters of high energy in the lattice. For $T \approx T_N$, the lattice is completely disordered. The same is true for $T = 2.5$ above T_N .

We shall now calculate the number of clusters and their sizes as a function of T in order to analyze the temperature-dependent behavior of the spin current.

The scattering by clusters in the Ising case in our previous model¹⁹ is now replaced in the Heisenberg spin model studied here, by a scattering due to large domain walls. Counting the number of clusters in the Heisenberg case requires some particular attention, as seen in the following.

(1) We equilibrate the system at T . (2) We generate first bonds according to the algorithm by Wolff:^{29,30} this consists in replacing the two spins, where the link is verified by the Wolff probability, by their larger value (Fig. 2). (3) Next we discretize S_z , the z component of each spin, into values between -1 and 1 , with a step 0.1 . (4) Only then can we use the algorithm of Hoshen-Kopelman to form a cluster with neighboring spins of the same S_z . This is how our clusters in the Heisenberg case are obtained.

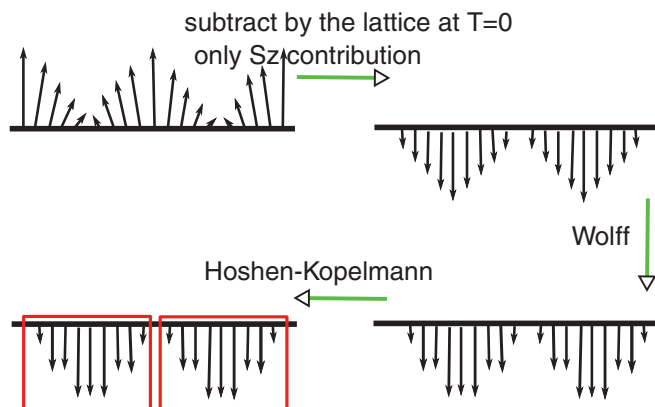


FIG. 2. (Color online) The successive steps in the application of the algorithm by Wolff to the case of Heisenberg spin (see text for explanation).

Note that we can define a cluster distribution by each value of S_z . We can therefore distinguish the amplitude of scattering: as seen below, scattering is stronger for clusters with larger S_z . We have used the above procedure to count the number of clusters in our simulation of an antiferromagnetic thin film. In Fig. 3 we show the number of cluster η versus T for several values of S_z .

In addition, we have determined the average size of these clusters as a function of T . The results are shown in Fig. 4. One observes that the size and the number of clusters of any value of S_z change the behavior, showing a maximum at the transition temperature.

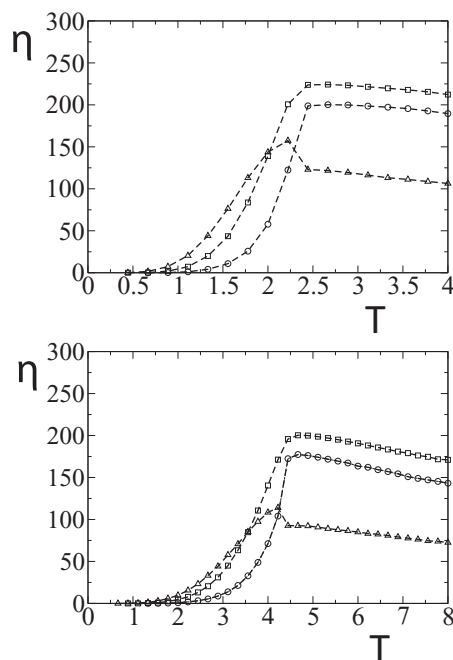


FIG. 3. Number of clusters versus temperature for anisotropy $A = 0.01$ (upper) and $A = 1$ (lower). The values of S_z are 1 , 0.8 , and 0.6 denoted by circles, squares, and triangles, respectively. Lines are guides to the eye.

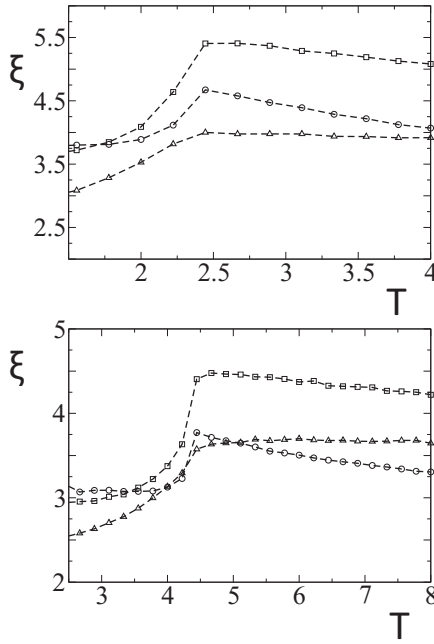


FIG. 4. Average size of clusters versus temperature for anisotropy $A = 0.01$ (upper) and $A = 1$ (lower). The values of S_z are 1, 0.8, and 0.6 denoted by circles, squares, and triangles, respectively. Lines are guides to the eye.

The resistivity, as mentioned above, indeed depends on the amplitude of S_z as seen in the expression

$$\rho = \frac{m}{ne^2} \frac{1}{\tau} = \frac{m}{ne^2} \sum_{i=-S_z}^{S_z} \frac{1}{\tau_i}. \quad (16)$$

III. RESULTS

A. Effect of Ising-like anisotropy

At this stage, it is worth reexamining some fundamental effects of V_0 and A . It is necessary to know acceptable values of V_0 imposed by the Born approximation. To do this we must calculate the resistivity with the second-order Born approximation:

$$\sigma_k^B(\theta, \phi) = \left| \frac{F(\theta, \phi)}{4\pi} \right|^2, \quad (17a)$$

$$F(\theta, \phi) = \frac{2m\Omega}{\hbar^2} \left[\int d^3r e^{-i\mathbf{K}\cdot\mathbf{r}} J(r) - \frac{1}{4\pi} \int d^3r e^{-i\mathbf{K}\cdot\mathbf{r}} \frac{J(r)}{r} \times \int d^3r' e^{-i\mathbf{K}\cdot\mathbf{r}'} J(r') \right], \quad (17b)$$

$$K = |\mathbf{k} - \mathbf{k}'| = k[2(1 - \cos \theta)]^{1/2} \text{ and } J(r) = V_0 e^{-r/\xi},$$

we find, with $D = \eta 32\pi \Omega m / \hbar^3$,

$$\frac{1}{\tau_k} = DV_0^2 k \left[\frac{2\xi^6}{[1 + (2\xi k)^2]^2} - \frac{V_0}{3[1 + (2\xi k)^2]^2} \times \left(1 + \frac{4}{[1 + (2\xi k)^2]^2} \right) + \frac{V_0^2 \xi^6}{12(2k)^2} \right]. \quad (18)$$

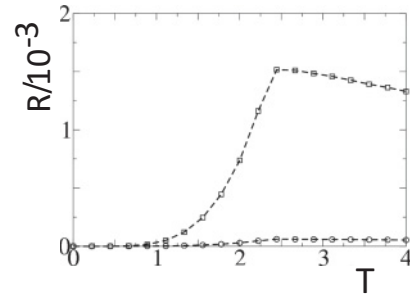


FIG. 5. Ratio $R = \rho(\text{Born2})/\rho(\text{Born1})$ versus T for $V_0=0.05$ (squares, upper curve) and 0.01 (circles, lower curve) (see text for comments).

The first term is due to the first order of Born approximation and the second and third terms are due to corrections from the second order. We plot $\rho(\text{Born2})/\rho(\text{Born1})$ versus T in Fig. 5 for different values of V_0 , $\rho(\text{Born1})$ and $\rho(\text{Born2})$ being, respectively, the resistivities calculated at first and second order. We note that the larger this ratio is, the more important the corrections due to the second order become. From Fig. 5, several remarks are in order: The first order of Born approximation is valid for small values of V_0 as seen in the case $V_0 = 0.01$, corresponding to a few meV. In this case, the correction does not depend on T . This is understandable because with such a weak coupling to the lattice, itinerant spins do not feel the second-order effect of the lattice spin disordering. In the case of strong V_0 , such as $V_0 = 0.05$, the second-order approximation should be used. Interestingly enough, the correction is strongly affected by T with a peak corresponding to the phase transition temperature of the lattice.

We now examine the effect of A . Figure 6 shows the variation of the sublattice magnetization and of T_N with anisotropy A . We have obtained, respectively, for $A = 0.01$, $A = 1$, $A = 1.5$, and the pure Ising case, the following critical temperatures $T_N \simeq 2.3, 4.6, 5.6$, and 6.0. Note that the pure Ising case has been simulated with the pure Ising Hamiltonian, not with Eq. (15) (we cannot use $A = \infty$). We can easily understand that not only the spin resistivity will follow this variation of T_N but also, the change of A will fundamentally alter the resistivity behavior as will be seen below.

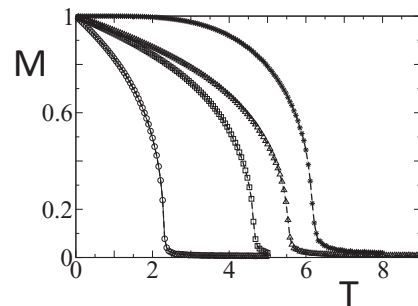


FIG. 6. Sublattice magnetization versus T for several values of anisotropy A . From left to right, $A = 0.01$, $A = 1$, $A = 1.5$, and pure Ising spin.

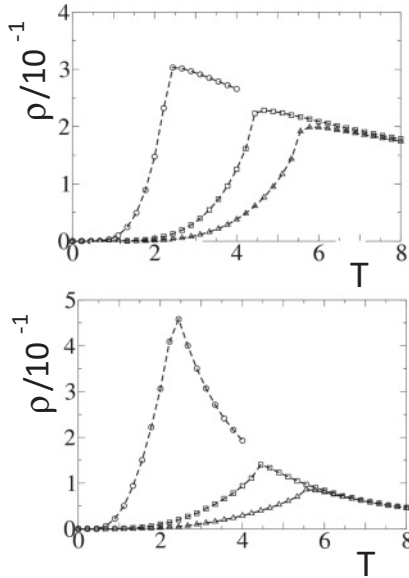


FIG. 7. Spin resistivity versus T for several anisotropy values A in an antiferromagnetic bcc system: $A = 0.01$ (circles), 1 (squares), and 1.5 (triangles). Upper (lower) curves: degenerate (nondegenerate) system.

The results shown in Fig. 7 clearly indicate the appearance of a peak at the transition which diminishes with increasing anisotropy. If we look at Fig. 4, which shows the average size of clusters as a function of T , we observe that the size of clusters of large S_z diminishes with increasing A .

We show in Fig. 8 the pure Heisenberg and Ising models. For the pure Ising model, there is just a shoulder around T_N with a different behavior in the paramagnetic phase: an increase or decrease with increasing T for degenerate or nondegenerate cases. It is worth mentioning that MC simulations for the pure Ising model on the simple cubic and bcc antiferromagnets where interactions between itinerant spins are taken into account in addition to Eq. (1), show no peak at all.^{31,32} These results are in agreement with the tendency observed here for increasing A .

B. Effect of magnetic field

We now apply a magnetic field perpendicularly to the electric field. To see the effect of the magnetic field, it suffices to replace the distribution function by

$$f_k^1 = \frac{e\hbar\tau_k}{m} \left(-\frac{\partial f^0}{\partial \epsilon} \right) \mathbf{k} \cdot \frac{(\mathbf{E} - \frac{e\tau_k}{mc} \mathbf{H} \wedge \mathbf{E})}{1 + \left(\frac{e\tau_k H}{mc} \right)^2}. \quad (19)$$

From this, we obtain the following equations for the contributions of up and down spins:

$$\rho_\downarrow = \sum_{S_z=-1}^{+1} (S_z + 1)^2 \frac{\eta 4V_0^2 m^2 \pi k_f \xi^2}{ne^2 \hbar^3} \left[\frac{4\xi^2}{1 + 4\xi^2 k_f^2} \right]^2, \quad (20)$$

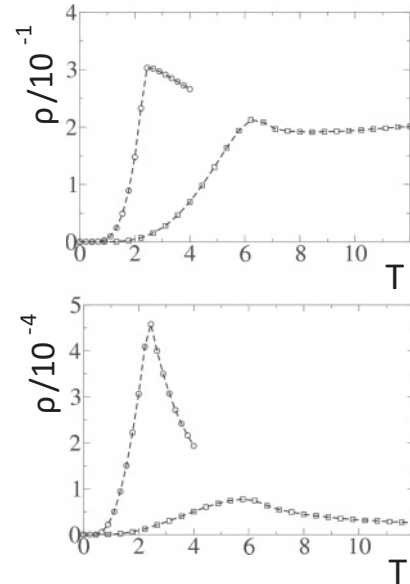


FIG. 8. Spin resistivity for pure Heisenberg (circles) and Ising (squares) models in an antiferromagnetic bcc system. Upper (lower) curves: degenerate (nondegenerate) system.

$$\rho_\uparrow = \sum_{S_z=-1}^{+1} (S_z - 1)^2 \frac{\eta 4V_0^2 m^2 \pi k_f \xi^2}{ne^2 \hbar^3} \left[\frac{4\xi^2}{1 + 4\xi^2 k_f^2} \right]^2, \quad (21)$$

where S_z is the domain-wall spin (scattering centers) and V_0 is the coefficient of the exchange integral between an itinerant spin and a lattice spin [see Eq. (8)].

Figures 9 and 10 show the resistivity for several magnetic fields. We observe a split in the resistivity for up and down spins which is larger for stronger fields. Also, we see that the minority spins show a smaller resistivity due to their smaller number. The reason for this is similar to the effect of A mentioned above and can be understood by examining Fig. 11, where we show the evolution of the number and the average size of clusters with the temperature in a magnetic field. By comparing with the zero-field results shown in Figs. 3 and 4, we can see that while the number of clusters does not change with the applied field, the size of clusters is significantly bigger. It is easy to understand this situation: when we apply a magnetic field, the spins want to align themselves to the field so the up-spin domains become larger, critical fluctuations are at least partially suppressed, and the transition is softened.

Before showing the application to hexagonal MnTe, let us make a few remarks:

(i) We have chosen a presentation of the general model which can be applied to degenerate and nondegenerate semiconductors and semimetals. In the degenerate case, k_f depends only on the carrier concentration n via the known formula $k_f = (3\pi^2 n)^{1/3}$;

(ii) In semiconductors, the carrier concentration is a function of T . In our model, we suppose that the number of itinerant spins is independent of T in each simulation. However, in each simulation, we can take another concentration (see

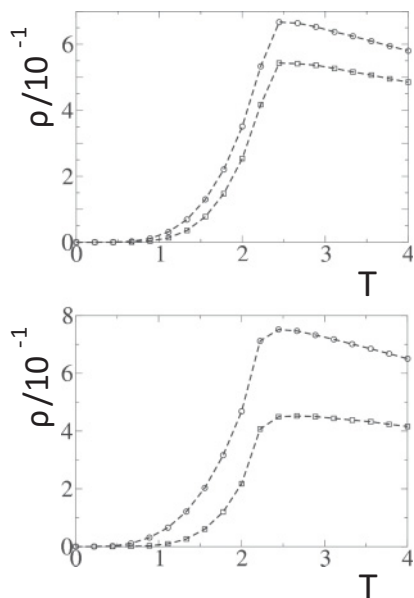


FIG. 9. Resistivities of up (circles) and down (squares) spins versus T for two magnetic field's strengths in the degenerate case. Top (bottom): $B = 0.6$ (1.5).

Ref. 19): the results show that the resistivity is not strongly modified; one still has the same feature, except that the stronger the concentration is, the smaller the peak at T_C becomes if and only if interaction between itinerant spins is taken into account. Therefore, we believe that generic effects independent of carrier concentration will remain. Of course, the correct way is to use a formula to generate the carrier concentration as a function of T and to make the simulation with the temperature-dependent concentration taking account of additional scattering due to interaction between itinerant

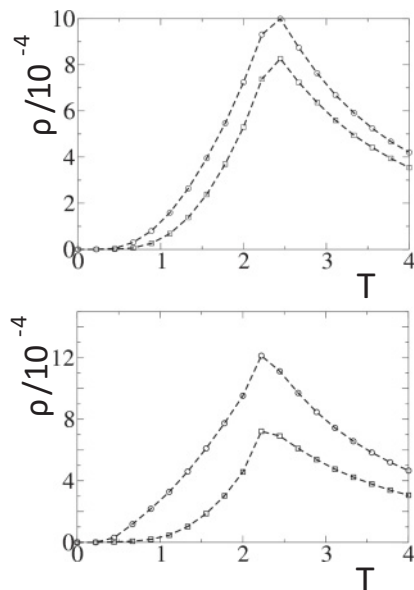


FIG. 10. Resistivities of up (circles) and down (squares) spins versus T for two magnetic field's strengths in the nondegenerate case. Top (bottom): $B = 0.6$ (1.5).

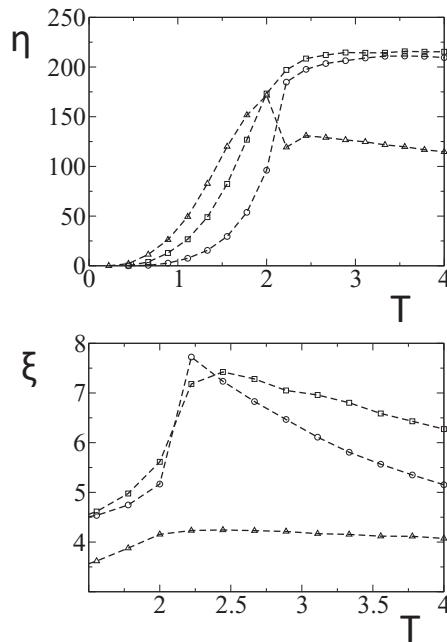


FIG. 11. Upper: number of clusters; lower: average size of clusters, versus T for several values of S_z and for magnetic field $B = 1.5$; circles: $S_z = 1$; squares: $S_z = 0.8$; and triangles: $S_z = 0.6$. Lines are guides to the eye.

spins. Unfortunately, to obtain that formula we have to use several approximations which involve more parameters. We will try this in a future work.

C. Application to MnTe

We now apply our formulas to MnTe. The pure MnTe crystallizes in either the zinc-blende structure³³ or the hexagonal NiAs structure³⁴ (see Fig. 12). MnTe is a well-studied p -type semiconductor with numerous applications due to its high Néel

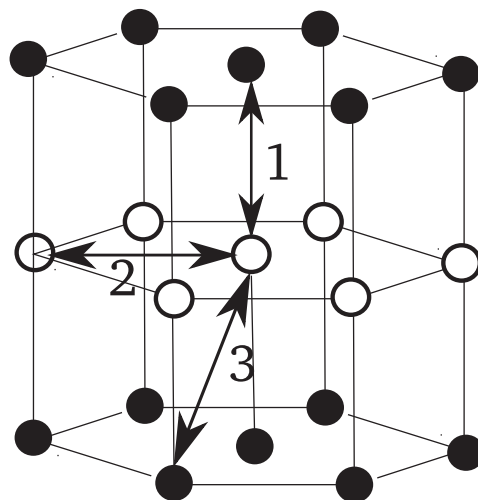


FIG. 12. Structure of the type NiAs is shown with Mn atoms only. This is a stacked hexagonal lattice. Up spins are shown by black circles, down spins by white ones. Nearest-neighbor (NN) bond is marked by 1, next NN bond by 2, and third NN bond by 3.

temperature. We are interested here in the case of hexagonal structure. For this case, the Néel temperature is $T_N = 310$ K.³⁴ Hexagonal MnTe is a crossroad semiconductor with a big gap (1.27 eV) and a room-temperature carrier concentration of $n = 4.3 \times 10^{17} \text{ cm}^{-3}$.³⁵ Without doping, MnTe is nondegenerate. In doped cases,^{36–39} band tails created by doped impurities can cover, more or less, the gap. But these systems, which are disordered by doping, are not a purpose of our present study. So, in the following we apply the nondegenerate formulas to MnTe.

Magnetic properties are determined mainly by an anti-ferromagnetic exchange integral between NN Mn along the c axis, namely, $J_1/k_B = -21.5 \pm 0.3$ K, and a ferromagnetic exchange, $J_2/k_B \approx 0.67 \pm 0.05$ between in-plane (next NN) Mn. The third NN interaction has also been measured with $J_3/k_B \approx -2.87 \pm 0.04$ K. Note that the spins are lying in the xy planes perpendicular to the c direction, with an in-plane easy-axis anisotropy.³⁴ The magnetic structure is therefore composed of ferromagnetic xy hexagonal planes antiferromagnetically stacked in the c direction. The NN distance in the c direction is therefore $c/2 \approx 3.36$ shorter than the in-plane NN distance a . The cell parameters are $a = 4.158$ Å and $c = 6.71$ Å.

We have calculated the cluster distribution for the hexagonal MnTe using the exchange integrals taken from Ref. 34 and the other crystal parameters taken from the literature.^{40–42} The result is shown in Fig. 13. The spin resistivity in MnTe obtained with our theoretical nondegenerate model is presented in Fig. 14 for a density of itinerant spins corresponding to $n = 4.3 \times 10^{17} \text{ cm}^{-3}$,³⁵ together with “normalized” experimental data. The normalization has been made by noting that the experimental resistivity R in Ref. 42 is the total one with contributions from impurities and phonons. However, the

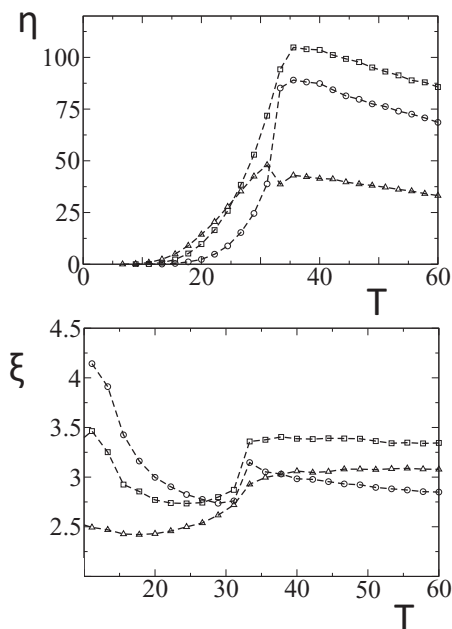


FIG. 13. Number of clusters (upper) and cluster size (lower) versus T for the MnTe structure obtained from Monte Carlo simulations for several values of S_2 : 1 (circles), 0.8 (squares), and 0.6 (triangles). Lines are guides to the eye.

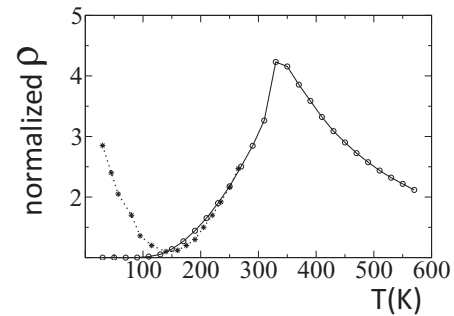


FIG. 14. Normalized spin resistivity versus T in MnTe: theoretical nondegenerate case (circles) and experimental results (stars) from Chandra *et al.*⁴² Experimental data lie on the theoretical line for $T \geq 140$ K (see text for comments).

phonon contribution is important only at high T , so we can neglect it for $T < 310$ K. For the contribution R_0 from fixed impurities, there are reasons to consider it as temperature independent at low T . From these rather rude considerations, we extract R_0 from R and compare our theoretical value with $R - R_0$. This is what we called “normalized resistivity” in Fig. 14.

Several remarks are in order:

(i) The peak temperature of our theoretical model is found at 325 K, a little bit higher than the the experimental Néel temperature given in Refs. 34 and 42, but very close to 323 K given in Ref. 35.

(ii) Our result is in agreement with experimental data obtained by Chandra *et al.*⁴² for temperatures between 140 and 280 K, above which Chandra *et al.* did not, unfortunately, measure.

(iii) At temperatures lower than 140 K, the experimental curve increases with decreasing T . Note that many experimental data on various materials show this “universal” feature: we can mention the data by Li *et al.*,¹⁶ Du *et al.*,¹² Zhang *et al.*,¹³ McGuire *et al.*,²⁵ among others. Our theoretical model based on the scattering by defect clusters cannot account for this behavior because there are no defects at very low T . Direct MC simulation shows, however, that the freezing indeed occurs at low T both in ferromagnets^{19,31} and antiferromagnets,³² giving rise to an increase of the spin resistivity with decreasing T . There are several explanations for this experimental behavior, among which we can mention the fact that in semiconductors, the carrier concentration increases as T increases, giving rise to an increase of the spin current, namely, a decrease of the resistivity, with increasing T in the low- T region. Another origin of the increase of ρ as $T \rightarrow 0$ is the possibility that the itinerant electrons may be frozen (crystallized) due to their interactions with localized spins and between themselves, giving rise to a low mobility. On the hypothesis of frozen electrons, there is a reference on the charge ordering at low T in $\text{Pr}_{0.5}\text{Ca}_{0.5}\text{MnO}_3$ (Ref. 13) due to some strain interaction. A magnetic field can make this ordering melted, giving rise to a depressed resistivity. Our present model does not correspond to this compound but we believe that the concept is similar. For the system $\text{Pr}_{0.5}\text{Ca}_{0.5}\text{MnO}_3$, which shows a commensurate charge order,

the “melting” fields at low temperatures are high, on the order of 25 T.¹³

(iv) The existence of the peak at $T_N \simeq 325$ K of the theoretical spin resistivity shown in Fig. 14 is in agreement with experimental data recently published by Li *et al.*¹⁶ (see the inset of their Fig. 5). Unfortunately, we could not renormalize the resistivity values of Li *et al.*¹⁶ to put in the same figure with our result for a quantitative comparison. Other data on various materials^{12,13,25} also show a large peak at the magnetic transition temperature.

To close this section, let us note that it is also possible, with some precaution, to apply our model on other families of antiferromagnetic semiconductors such as CeRhIn₅ and LaFeAsO. An example of supplementary difficulties but exciting subjects encountered in the latter compound is that there are two transitions in a small temperature region: a magnetic transition at 145 K and a tetragonal-orthorhombic crystallographic phase transition at 160 K.^{25,26} An application to ferromagnetic semiconductors of n -type CdCr₂Se₄ (Ref. 43) is under way. In the case of Cd_{1-x}Mn_xTe, the question of the crystal structure, depending on the doping concentration x , remains open. Cd_{1-x}Mn_xTe can have one of the following structures, the NiAs structure, the zinc-blende one, or a mixed phase.³⁶⁻³⁹

IV. CONCLUSION

In this paper, we have shown the behavior of the magnetic resistivity ρ as a function of temperature in antiferromagnetic semiconductors. The main interaction that governs the resistivity behavior is the interaction between itinerant spins and the

lattice spins. Our analysis is based on the Boltzmann equation, which uses the temperature-dependent cluster distribution obtained by MC simulation. Our result is in agreement with the theory by Haas:²¹ we observe a broad maximum of ρ in the temperature region of the magnetic transition without a sharp peak observed in ferromagnetic materials. We have studied the two cases, degenerate and nondegenerate semiconductors. The nondegenerate case shows a maximum which is more pronounced than that of the degenerate case. We would like to emphasize that the shape of the maximum and its existence depend on several physical parameters such as interactions between different kinds of spins, the spin model, the crystal structure, etc.

In this paper we applied our theoretical nondegenerate model to the antiferromagnetic semiconductor MnTe. We found good agreement with experimental data below the transition region. We note, however, that our model using the cluster distribution cannot be applied at very low T where the spin resistivity in experiments is dominated by effects other than the $s-d$ scattering model of the present paper. One of these possible effects is the carrier proliferation with increasing temperatures in semiconductors, which makes the resistivity decrease with increasing T , experimentally observed in magnetic semiconductors at low T .

ACKNOWLEDGMENTS

One of us (K.A.) wishes to thank the JSPS for the financial support of his stay at Okayama University where this work was carried out. He is also grateful to the researchers of Isao Harada’s group for helpful discussions.

*Corresponding author: diep@u-cergy.fr.

¹T. Kasuya, *Prog. Theor. Phys.* **16**, 58 (1956).

²G. Zaránd, C. P. Moca, and B. Janko, *Phys. Rev. Lett.* **94**, 247202 (2005).

³P.-G. de Gennes and J. Friedel, *J. Phys. Chem. Solids* **4**, 71 (1958).

⁴M. E. Fisher and J. S. Langer, *Phys. Rev. Lett.* **20**, 665 (1968).

⁵M. Kataoka, *Phys. Rev. B* **63**, 134435 (2001).

⁶A. L. Wysocki, R. F. Sabirianov, M. van Schilfhaarde, and K. D. Belashchenko, *Phys. Rev. B* **80**, 224423 (2009).

⁷F. Matsukura, H. Ohno, A. Shen, and Y. Sugawara, *Phys. Rev. B* **57**, R2037 (1998).

⁸A. E. Petrova, E. D. Bauer, V. Krasnorussky, and S. M. Stishov, *Phys. Rev. B* **74**, 092401 (2006).

⁹F. C. Schwerer and L. J. Cuddy, *Phys. Rev.* **2**, 1575 (1970).

¹⁰J. Xia, W. Siemons, G. Koster, M. R. Beasley, and A. Kapitulnik, *Phys. Rev. B* **79**, 140407(R) (2009).

¹¹C. L. Lu, X. Chen, S. Dong, K. F. Wang, H. L. Cai, J.-M. Liu, D. Li, and Z. D. Zhang, *Phys. Rev. B* **79**, 245105 (2009).

¹²J. Du, D. Li, Y. B. Li, N. K. Sun, J. Li, and Z. D. Zhang, *Phys. Rev. B* **76**, 094401 (2007).

¹³Y. Q. Zhang, Z. D. Zhang, and J. Aarts, *Phys. Rev. B* **79**, 224422 (2009).

¹⁴X. F. Wang, T. Wu, G. Wu, H. Chen, Y. L. Xie, J. J. Ying, Y. J. Yan, R. H. Liu, and X. H. Chen, *Phys. Rev. Lett.* **102**, 117005 (2009).

¹⁵T. S. Santos, S. J. May, J. L. Robertson, and A. Bhattacharya, *Phys. Rev. B* **80**, 155114 (2009).

¹⁶Y. B. Li, Y. Q. Zhang, N. K. Sun, Q. Zhang, D. Li, J. Li, and Z. D. Zhang, *Phys. Rev. B* **72**, 193308 (2005).

¹⁷K. Akabli, H. T. Diep, and S. Reynal, *J. Phys.: Condens. Matter* **19**, 356204 (2007).

¹⁸K. Akabli and H. T. Diep, *J. Appl. Phys.* **103**, 07F307 (2008).

¹⁹K. Akabli and H. T. Diep, *Phys. Rev. B* **77**, 165433 (2008).

²⁰Y. Suezaki and H. Mori, *Prog. Theor. Phys.* **41**, 1177 (1969).

²¹C. Haas, *Phys. Rev.* **168**, 531 (1968).

²²Y. Shapira and T. B. Reed, *Phys. Rev. B* **5**, 4877 (1972).

²³H. W. Lehmann, *Phys. Rev.* **163**, 488 (1967).

²⁴G. J. Snyder, T. Caillat, and J.-P. Fleurial, *Phys. Rev. B* **62**, 10185 (2000).

²⁵M. A. McGuire, A. D. Christianson, A. S. Sefat, B. C. Sales, M. D. Lumsden, R. Jin, E. A. Payzant, D. Mandrus, Y. Luan, V. Keppens, V. Varadarajan, J. W. Brill, R. P. Hermann, M. T. Sougrati, F. Grandjean, and G. J. Long, *Phys. Rev. B* **78**, 094517 (2008).

²⁶A. D. Christianson, A. H. Lacerda, M. F. Hundley, P. G. Pagliuso, and J. L. Sarrao, *Phys. Rev. B* **66**, 054410 (2002).

²⁷J. Hoshen and R. Kopelman, *Phys. Rev. B* **14**, 3438 (1974).

²⁸D. P. Landau and K. Binder, in *Monte Carlo Simulation in Statistical Physics*, edited by K. Binder and D. W. Heermann (Springer-Verlag, New York, 1988), p. 58.

- ²⁹U. Wolff, *Phys. Rev. Lett.* **62**, 361 (1989).
- ³⁰U. Wolff, *Phys. Rev. Lett.* **60**, 1461 (1988).
- ³¹Y. Magnin, K. Akabli, H. T. Diep, and I. Harada, *Comput. Mater. Sci.* **49**, S204 (2010).
- ³²Y. Magnin, K. Akabli, and H. T. Diep, *Phys. Rev. B* **83**, 144406 (2011).
- ³³B. Hennion, W. Szuszkiewicz, E. Dynowska, E. Janik, and T. Wojtowicz, *Phys. Rev. B* **66**, 224426 (2002).
- ³⁴W. Szuszkiewicz, E. Dynowska, B. Witkowska, and B. Hennion, *Phys. Rev. B* **73**, 104403 (2006).
- ³⁵J. W. Allen, G. Locovsky, and J. C. Mikkelsen Jr., *Solid State Commun.* **24**, 367 (1977).
- ³⁶N. G. Szwacki, E. Przezdziecka, E. Dynowska, P. Boguslawski, and J. Kossut, *Acta Phys. Pol. A* **106**, 233 (2004).
- ³⁷T. Komatsubara, M. Murakami, and E. Hirahara, *J. Phys. Soc. Jpn.* **18**, 356 (1963).
- ³⁸S.-H. Wei and A. Zunger, *Phys. Rev. B* **35**, 2340 (1987).
- ³⁹K. Adachi, *J. Phys. Soc. Jpn.* **16**, 2187 (1961).
- ⁴⁰M. Inoue, M. Tanabe, H. Yagi, and T. Tatsukawa, *J. Phys. Soc. Jpn.* **47**, 1879 (1979).
- ⁴¹T. Okada and S. Ohno, *J. Phys. Soc. Jpn.* **55**, 599 (1985).
- ⁴²S. Chandra, L. K. Malhotra, S. Dhara, and A. C. Rastogi, *Phys. Rev. B* **54**, 13694 (1996).
- ⁴³H. W. Lehmann and G. Harbeke, *J. Appl. Phys.* **38**, 946 (1967).